Revised manuscript
ID ic-2016-03117a

*Inorganic Chemistry*

# Circularly polarized luminescence of silica-grafted europium chiral derivatives prepared through a sequential functionalization

Lidia Armelao,[†§] Daniela Belli Dell'Amico,[‡] Luca Bellucci,[‡] Gregorio Bottaro,[†] Lorenzo Di Bari[‡*] Luca Labella,[‡*] Fabio Marchetti,[‡] Simona Samaritani[‡] and Francesco Zinna[‡a]

[‡]*Dipartimento di Chimica e Chimica Industriale, Università di Pisa and CIRCC, via Giuseppe Moruzzi 13, I-56124*

[§]*Dipartimento di Scienze Chimiche, Università di Padova, via Marzolo 1,I-35131*

[†]*CNR ICMATE and INSTM, Dipartimento di Scienze Chimiche, Università di Padova, via Marzolo 1,I-35131*

[a]*Current address: Department of Organic Chemistry, University of Geneva, Quai Ernest-Ansermet 30, CH-1211 Geneva 4, Switzerland*

## ABSTRACT

We describe a new organic/inorganic material emitting circularly polarized luminescence (CPL). The hybrid system was obtained by the following steps: *i)* preliminary grafting of the europium *N*,*N*-dibutylcarbamate [$Eu(O_2CNBu_2)_3$] complex onto silica, *ii)* substitution of the residual carbamato groups with anionic 1,3-diphenyl-1,3-propanedionato ligands (dbm), and *iii)* subsequent introduction of the neutral tridentate chiral ligand 2,6-bis[isopropyl-2-oxazolin-2-yl]-pyridine ($^{i}$Pr-PyBox) in the metal coordination sphere. The solid material is stable to air and does not leach either the metal or the ligand. Samples of both the enantiomers have been studied showing mirror image CPL spectra. The molecular compounds [$Eu(dbm)_3$(*S*)-($^{i}$Pr-PyBox)] and [$Eu(dbm)_3$(*R*)-($^{i}$Pr-PyBox)] were prepared for comparison purposes and their molecular structures studied by single crystal X-ray diffraction showing mononuclear derivatives with a coordination number nine for europium. Powder-XRD showed a single crystalline phase. Photoluminescence and CPL evidenced the presence of a single emitting species.

## INTRODUCTION

The chemistry of lanthanide elements continues to play a pivotal role in the development of both molecular and materials science.[1] Particularly, in modern science and technology, the synthesis of asymmetric lanthanide complexes is an important issue both in catalysis[2] and for

their unique luminescent properties.[3] A special interest is continuously rising for circularly polarized luminescence (CPL) of chiral lanthanide complexes:[4] if the system is properly designed, extremely high degrees of circular polarization in emission can be obtained.[5]

For such properties, chiral lanthanide systems are currently employed as probes for (bio)-molecules,[6] or as the guest emitters in OLEDs able to directly emit highly circularly polarized electroluminescence.[7]

Some of us recently developed a method to graft lanthanide(III) ions onto the surface of inorganic materials, thereby modifying their residual coordination sphere with functional organic ligands. Our method utilizes *N*,*N*-dialkylcarbamato complexes $[M(O_2CNR_2)_nL_m]$ for grafting metal ions both of *d* and *f* blocks onto silica or other inorganic oxides.[8] These complexes are an attractive alternative to organometallic precursors[9] since they are easy to prepare (especially in the case of lanthanides) and generally highly soluble in non-polar solvents. Moreover, they show a prompt reactivity toward protic agents releasing carbon dioxide and amine (Eq. 1). Among protic acids, also Brønsted acid sites on a material surface can react with substitution of one or more carbamato ligands per metal center, in dependence of the protic site proximity (Eq. 2).[10.]

$$[M(O_2CNR_2)_nL_m] + n\,HA \rightarrow MA_nL_m + n\,CO_2 + n\,NHR_2 \qquad (1)$$

$$\#\#\#\text{-}H + [M(O_2CNR_2)_nL_m] \rightarrow \#\#\#\text{-}M(O_2CNR_2)_{(n-1)}L_m + CO_2 + HNR_2 \qquad (2)$$

### represents the support surface

The residual carbamato groups can be easily displaced by protolytic substitution and replaced by ligands suitable to hit the desired target. By so doing, it is possible to transfer the peculiar properties of molecular metal complexes, like for instance their reactivity or their optical features, onto the material surface where they are dispersed. In our previous report8[i] we demonstrated that, through the application of this synthetic sequential approach to rare earth complexes, highly luminescent silica based materials could be achieved exploiting the brilliant and sharp *f*-*f* sensitized emissions of $Ln^{3+}$ ions. The grafting of $[Tb(O_2CNBu_2)_3]$ to silica was observed to produce a $CO_2$ evolution corresponding to a $CO_2$/Tb molar ratio of about 1. IR and XPS studies on the obtained silica confirmed the presence of residual carbamato ligands after grafting. Moreover, after treatment of the material with Hdbm, accompanied by $CO_2$ evolution, XPS and PL data supported the evidence of the protolytic substitution of the coordinated carbamato ligands by the β-diketonato ions.

A further challenge in this line is represented by the introduction of a chiral ligand, able to provide the necessary dissymmetric environment to elicit CPL. Indeed, there are only very few reports of nano-structured and organic/inorganic hybrid functional materials endowed with circularly polarized luminescence, such as CPL-active CdS quantum dots[11] or Tb complexes embedded in $SiO_2$ xerogel[12] or zirconium phosphate/phosphonate matrices.[13] To the best of our knowledge there is no report on CPL of materials containing Eu grafted onto an inorganic surface.

Here we show that a CPL emitting material can be prepared by following our versatile protocol with the addition of a further step where the coordinative demand of the metal centers is saturated by a chiral neutral ligand. Lanthanides show usually high coordination numbers (7-9) subject to a certain flexibility in dependence of the ligand peculiarities. Europium *N*,*N*-dibutylcarbamate, $[Eu(O_2CNBu_2)_3]$, was used as precursor to graft the metal to the silica surface and the residual carbamato ligands were then substituted by reaction with 1,3-diphenyl-1,3-propanedione (Hdbm). The sequence was finalized with the addition of the neutral 2,6-bis[isopropyl-2-oxazolin-2-yl]-pyridine ($^{i}$Pr-PyBox) as chiral inducer. The success of these consecutive steps was confirmed by photoluminescence (PL) and CPL measurements, and validated by the preparation and complete characterization of both enantiomers of the molecular species $[Eu(dbm)_3(^{i}Pr\text{-}PyBox)]$.

**Experimental Section**

**Materials and instrumentations.** All manipulations were performed in anhydrous conditions under a dinitrogen atmosphere. $[Eu(O_2CNBu_2)_3]$[14] and $[Eu(dbm)_3]$ [8i] were prepared as described in the literature. 2,6-bis[(4*S*)-isopropyl-2-oxazolin-2-yl]pyridine [(*S*)-$^{i}$Pr-PyBox (Aldrich, 99%)], 2,6-Bis[(4*R*)-isopropyl-2-oxazolin-2-yl]pyridine [(*R*)-$^{i}$Pr-PyBox (Aldrich, 99%)], 1,3-diphenyl-1,3-propanedione [Hdbm, (Fluka)] were used without further purification. Commercial silica (Grace, EP 17G, surface area 325 $m^2\ g^{-1}$, pore volume 1.82 $cm^3\ g^{-1}$, irregular particles of size in the range 60-20 μm) was treated at 160 °C over $P_4O_{10}$ for 20 h under vacuum up to a constant weight and then stored in flame-sealed vials under dry $N_2$ atmosphere. On the basis of our past experience,8[a,b] this type of pretreatment eliminates most of the hydrogen-bonded water from the surface, leaving most of the hydroxyl groups (Si-OH) which are chemically reactive towards metal precursors. The total silanol content (2.02 mmol $g^{-1}$) was estimated from mass loss upon further heating at 850°C.

ICP analyses were carried out with a Quadropole X7 ICP-MS ThermoFisher instrument.

A rare-earth multi-element standard containing europium (Inorganic Venture) was used. Samples were mineralized by acid attack ($HNO_3$).

SEM-EDX analyses were carried out with a FEI Quanta FEG-450 microscope supplied with a Philips XL 30 instrument. Sample disks were prepared by pressing the powders in a Specac manual hydraulic press.

Attenuated total reflectance-Fourier transform infrared spectroscopy (ATR-FTIR) spectra in the solid state were recorded with a PerkinElmer "Spectrum One" spectrometer. Volumetric analyses of the lanthanide content via EDTA complexometry were carried out on the filtrates of the grafting and functionalization processes.[15] The luminescence spectra were recorded on sample powders at room temperature in a front-face acquisition geometry with a spectrofluorimeter (Fluorolog-3, Horiba Jobin Yvon) equipped with double-grating monochromator in both the excitation and emission sides coupled to a R928P Hamamatsu photomultiplier and a 450 W Xe arc lamp as the excitation source. The emission spectra were corrected for detection and optical spectral response of the spectrofluorimeter supplied by the manufacturer. The excitation spectra were corrected for the spectral distribution of the lamp intensity using a photodiode reference detector. The luminescence lifetimes in the microsecond–millisecond scales were measured by a pulsed Xe lamp with variable repetition rate and elaborated with standard software fitting procedures. The experimental uncertainty on $\tau$ values is ±10%. Circularly Polarized Luminescence spectra were measured using a home-made instrument, described elsewhere,[16] using diffuse 365 nm excitation from a 20 cm mercury fluorescent tube ensuring isotropic illumination of the whole solid sample. The measurements were carried out on depositions prepared by suspending the silica samples in toluene and depositing the resulting slurry onto a quartz plate. For each deposition, several spectra were acquired after rotating the sample (by 90°, 180° around the optical axis and by flipping it front to back, to record both faces). These spectra did not differ significantly, confirming that no artifact due to linearly polarized components was present in the film. All the spectra were normalized to the corresponding luminescence intensity of the $^5D_0 \rightarrow {}^7F_2$ band in the emission spectrum (measured simultaneously with CPL) and then averaged. The dissymmetry factor *g* was calculated according to the definition, see below.

Acquisition parameters: time constant: 4 sec; scan-speed: 0.2 nm/sec; PMT voltage: 750 V.

The CPL of molecular species was measured on depositions prepared by dissolving completely the samples in $CH_2Cl_2$ and drop-casting the solution onto a quartz plate. The same acquisition and data analysis protocol detailed above was followed.

**Grafting of [Eu($O_2CNBu_2$)$_3$] on silica.** A pale yellow solution of [Eu($O_2CNBu_2$)$_3$] (5.51 g, 8.25 mmol) in toluene (100 mL) was reacted under dinitrogen atmosphere with $SiO_2$ (7.76 g) The suspension was stirred for 3 days under dinitrogen atmosphere, repeating vacuum/dinitrogen cycles. The solid was then filtered, washed with toluene (2 × 10 mL) and dried *in vacuo* at room temperature. The product was labeled as **SIL1**. ATR-FTIR (bands in the range 1700-1250 $cm^{-1}$): 1495, 1430, 1379, 1325. Analysis of the metal content of the pale yellow filtrate could establish that about 0.53 mmol per gram of silica had been loaded.

**Functionalization of SIL1 with Hdbm and (*R*)-$^{i}$Pr-PyBox or (*S*)-$^{i}$Pr-PyBox.** A sample of silica functionalized with europium, **SIL1**, (0.15 g, 0.08 mmol of Eu) was suspended in toluene (5 mL) and reacted with Hdbm (0.04 g, 0.18 mmol). The suspension turned to light-yellow with carbon dioxide evolution. After 24 h stirring, regularly repeating vacuum/dinitrogen cycles, the suspension was filtered. The solid was then suspended in fresh toluene (5 mL) and (*R*)-$^{i}$Pr-PyBox (0.02 g, 0.10 mmol) was added. The bright yellow suspension was stirred for 24 h and then filtered. The filtrate contained only traces of metal. The solid was washed with toluene (2 x 3 mL) and dried *in vacuo* at room temperature. Europium content was assessed by ICP analysis and corresponded to 0.65(±0.08) mmol Eu/g $SiO_2$. The product was labeled as **SIL2R**. ATR-FTIR (bands in the range 1700-1250 $cm^{-1}$): 1600, 1558, 1519, 1480, 1422, 1385. The same procedure was repeated using (*S*)-$^{i}$Pr-PyBox. In this case, **SIL1** (0.21 g, 0.10 mmol of Eu) was suspended in toluene (5 mL) and reacted with Hdbm (0.05 g, 0.20 mmol). After 24 h of vigorous stirring the solid was filtered and suspended in fresh toluene (5 mL) with (*S*)-$^{i}$Pr-PyBox (0.03 g, 0.10 mmol). The bright yellow suspension was stirred for 24 h and filtered. No metal leaching was observed in the filtrate. The solid, labeled as **SIL2S**, was washed with toluene (2 × 3 mL) and dried *in vacuo* at room temperature. Europium content was assessed by ICP analysis and corresponded to 0.62(±0.08) mmol Eu/g $SiO_2$. ATR-FTIR (bands in the range 1700-1250 $cm^{-1}$): 1601, 1556, 1519, 1480, 1462, 1407. PL and CPL studies were carried out for both the enantiomer forms of the functionalized sample. EDX measurements on both **SIL2R** and **SIL2S** revealed the presence of Eu, N and C in the approximate 1:2:43 molar ratio.

**Synthesis of [Eu(dbm)$_3$($^{i}$Pr-PyBox)].** [Eu(dbm)$_3$] (0.16 g, 0.19 mmol) was dissolved in toluene (20 mL) and (*S*)-$^{i}$Pr-PyBox (0.06 g, 0.20 mmol) was added to the yellow solution. After two hour stirring at room temperature the solution was concentrated, the bright yellow product was precipitated adding heptane (10 mL) and dried *in vacuo* (0.15 g; 0.13 mmol 68%

yield). Anal. Calcd for $C_{62}H_{56}N_3EuO_8$: C, 66.3; H, 5.0; N, 3.7. Found: C, 66.2; H, 4.7; N, 3.6. ATR-FTIR (bands in the range 1700-1250 $cm^{-1}$): 1599, 1557, 1514, 1477, 1456, 1405, 1368, 1305, 1273. The same procedure was repeated using (*R*)-$^{i}$Pr-PyBox. To a solution of $Eu(dbm)_3$ (0.43 g, 0.53 mmol) in toluene (40 mL), a stoichiometric amount of (*R*)-$^{i}$Pr-PyBox (0.16 g, 0.53 mmol) was added. After two hour stirring at room temperature the solution was concentrated to one third of the initial volume. The bright yellow product was precipitated adding heptane (10 mL), filtered and dried *in vacuo* (0.42 g; 0.37 mmol 71% yield). Anal. Calcd for $C_{62}H_{56}N_3EuO_8$: C, 66.3; H, 5.0; N, 3.7. Found: C, 66.2; H, 4,9; N, 3,7. ATR-FTIR (bands in the range 1700-1250 $cm^{-1}$): 1599, 1557, 1514, 1477, 1456, 1405, 1368, 1305, 1273. Both molecular compounds are air stable and quite soluble in toluene. PL and CPL studies were carried out for both the enantiomer forms.

**X-ray Diffraction studies.** Crystals of [$Eu(dbm)_3$(*S*)-($^{i}$Pr-PyBox)] and [$Eu(dbm)_3$(*R*)-($^{i}$Pr-PyBox)] were selected at room temperature (293 K), glued to glass fibers and analyzed with a Bruker Smart Breeze CCD diffractometer. Intensity data were collected up to a max $2\theta$ angle of 26.3 deg and 33.2 deg, respectively. Both the crystals have monoclinic symmetry and their diffraction patterns showed systematic extinctions due to a screw helix. The lattice parameters and some collection details are summarized in Table 1. The standard deviations coming from the collection software[17] are probably underestimated. After correction for Lorentz and polarization effects and for absorption, the structure solutions were obtained on both the data series using the direct methods contained in SHELXS program[18]. The asymmetric units of both crystal structures, consist of two independent molecules with slightly different conformations. The molecules present a europium ion coordinated by three dbm ligands and one $^{i}$Pr-PyBox ligand. During the structure refinement, the displacement parameters of the carbon atoms of a phenyl moiety of two dbm ligands and those of an isopropyl group of $^{i}$Pr-PyBox became too large, suggesting the presence of disorder. These moieties were finally refined as distributed in two limit positions fixing to one the total occupancy of the site. The final reliability factors and some details of the refinement procedure are listed in Table 1. The structure refinement calculations were carried out using SHELXL program;[19] other control calculations were performed with the programs contained in the suite WINGX.[20]

X-ray crystallographic data of [$Eu(dbm)_3$((S)-iPr-PyBox)] and [$Eu(dbm)_3$((R)-iPr-PyBox)] in CIF format (CCDC 1523915-1523916) can be obtained free of charge from the Cambridge Crystallographic Data Center, 12 Union Road, Cambridge CB2 1EZ, UK; fax: +44 1223 336 033; or e-mail: deposit@ccdc.cam.ac.uk.

**Table 1. Crystal data and structure refinements**

| Compound | **[Eu(dbm)$_3$(*S*)-(*i*Pr-PyBox)]** | **[Eu(dbm)$_3$(*R*)-(*i*Pr-PyBox)]** |
|---|---|---|
| chemical formula | $C_{62}H_{56}N_3O_8Eu$ | $C_{62}H_{56}N_3O_8Eu$ |
| fw | 1123.06 | 1123.06 |
| Crystal system | Monoclinic | Monoclinic |
| Space group | $P2_1$ (No. 4) | $P2_1$ (No. 4) |
| $a$, Å | 15.4298(8) | 15.4150(3) |
| $b$, Å | 20.8882(10) | 20.8733(5) |
| $c$, Å | 18.7141(9) | 18.6935(5) |
| $\beta$, deg | 114.0970(10) | 114.0700(10) |
| $V$, Å$^3$ | 5505.9(5) | 5491.8(2) |
| $Z$ | 4 | 4 |
| temp, K | 296(2) | 296(2) |
| $D_{calcd}$, g·cm$^{-3}$ | 1.355 | 1.358 |
| $\mu$, mm$^{-1}$ | 1.196 | 1.199 |
| $\vartheta_{max}$, deg | 26.284 | 33.161 |
| no. measured | 46705 | 74163 |
| no. unique [$R_{int}$] | 19079 [0.0323] | 37672 [0.0241] |
| no. parameters | 1459 | 1471 |
| $R_1$, $wR_2$ [$I>2\sigma(I)$] [a] | 0.0344, 0.0654 | 0.0388, 0.0817 |
| $R_1$, $wR_2$ [all data] [a] | 0.0700, 0.0756 | 0.0706, 0.0953 |
| absolut struct. parameter | –0.008(6) | –0.029(4) |
| goodness of fit [a] on $F^2$ | 0.985 | 1.007 |

[a] $R(F_o) = \Sigma\big||F_o|-|F_c|\big| / \Sigma|F_o|$; $Rw(F_o^2) = [\Sigma[w(F_o^2-F_c^2)^2] / \Sigma[w(F_o^2)^2]]^{½}$; $w = 1 / [\sigma^2(F_o^2) + (AQ)^2 + BQ]$ where $Q = [MAX(F_o^2,0) + 2F_c^2] / 3$; GOF = $[\Sigma[w(F_o^2-F_c^2)^2]/(N-P)]^{½}$, where $N$, $P$ are the numbers of observations and parameters, respectively

## Results and Discussion

The europium dibutylcarbamato derivative, $[Eu(O_2CNBu_2)_3]$, prepared in a convenient and high yield route according to a recently developed method,[14] is highly soluble in hydrocarbon solvents. It was reacted in toluene at room temperature, according to the protocol previously described for the analogous terbium derivative[8i] with a commercial silica thermally pre-treated to remove any adsorbed water. Carbon dioxide evolution can be noticed upon metal grafting. After filtration, the resulting europium loaded matrix was repeatedly washed with toluene to eliminate any metal center unbonded to the support. The metal covalently bonded to the inorganic surface retained in its coordination sphere unreacted carbamato ligands showing characteristic bands in the ATR-IR spectrum in the 1600–1300 cm$^{-1}$ region. The metal loading, estimated from the difference between the initially used amount and the metal content in the filtrate, was in keeping with previous experiments (around half a mmol per gram of silica). As previously reported for terbium,[8i] residual carbamato ligands were displaced using a weak protic agent as 1,3-diphenyl-1,3-propanedione (Hdbm) (pKa = 8.95). The protolysis occurs at room temperature with evolution of $CO_2$ and releasing of dibutylamine and the material obtained was washed several times and dried. The chosen ligand exemplifies here an efficient “antenna”, an excellent and widely used europium luminescence sensitizer.[21]

It is well known that lanthanide centers show a marked preference toward high coordination numbers without a strict preference towards a particular geometry so that variable coordination geometry is often dictated by the steric requirement of the ligands. Besides, since a β-diketonato ligand normally prefers a bidentate chelate coordination mode, it appeared possible to introduce a basic neutral multidentate ligand into the coordination sphere of the silica-grafted metal. Beyond a further functionalization of the surface, this achievement could minimize luminescence quenching mechanisms due to both the coordination of adventitious water or of proximal surface hydroxyl groups to the metal.

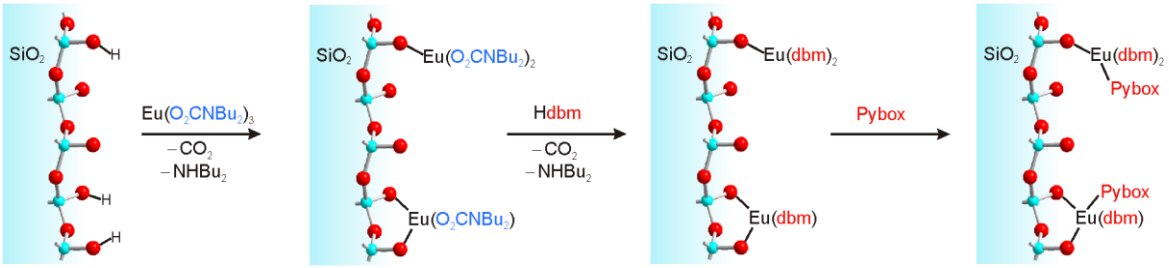


**Scheme 1.** A sketch of the grafting of an europium carbamato complex to a surface followed by further functionalizations: reaction with Hdbm and addition of $^{i}$Pr-PyBox.

The further functionalization of the inorganic surface was obtained here by coordinating a neutral chiral heteroaromatic base to the grafted metal centers. By adding one equivalent per $Eu^{3+}$ metal center of R or S enantiomer of 2,6-bis[isopropyl-2-oxazolin-2-yl]-pyridine [$^{i}$Pr-PyBox]4[a, 22] (Fig. 1) a material showing chiroptical emission properties was obtained.

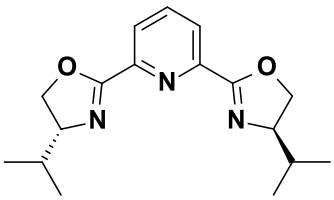


**Figure 1.** (*R*)-($^{i}$Pr-PyBox)

We used a PyBox/Eu molar ratio equal to 1 having confidence that also on the silica surface the addition of PyBox proceeds smoothly, as at molecular level (see below). Anyway, we cannot exclude the presence of europium ions uncoordinated to PyBox. Although the complexity of the system prevents a detailed description at the level of the europium coordination sphere and geometry at any depicted step, a sketch describing the chemical sequences of the grafting and functionalization processes is reported in Scheme 1

The europium content was checked by ICP analysis, corresponding to about 0.6 mmol of metal per gram of silica for both **SIL2R** and **SIL2S**. Moreover, SEM-EDX analysis showed a homogeneous distribution of europium on the surface and allowed an evaluation of the Eu:N:C molar ratios that resulted 1:2:43 for both species. These semi-quantitative data do not largely deviate from the expected values for a mixture of fragments of the type #SiO-Ln(dbm)$_2$(PyBox) and (#SiO-)$_2$Ln(dbm)(PyBox) on the surface. A nitrogen/europium ratio lower than expected can be due to the analytical limits of the employed method or to an incomplete coordination of PyBox to the europium centers. Indeed, poor accessibility of some sites could hamper the efficient interaction of the metal atoms with PyBox ligands.

As a matter of fact, a well measurable set of CPL signals could be observed from a deposition of the functionalized silica on a quartz plate, as shown in Fig. 2. The curves obtained for the two enantiomer samples (**SIL2S** and **SIL2R**) are mirror images as expected, confirming the reliability of the measurement. The CPL spectrum is very rich, which is due to the fact that different coordination environments around the metal center are present (see below, photophysical characterization). In particular, several bands with opposite sign are visible for the $^5D_0 \rightarrow {}^7F_2$ transition. The positive band (for **SIL2R**) at 621 nm, the positive shoulder (617 nm) and the intense positive band (612 nm) are allied with the multiplicity featured by the hypersensitive transition in the luminescence spectrum (Fig. 2).

In order to observe any chiroptical activity, the europium centers must interact with a chiral environment, which in our case is provided by the PyBox ligand, therefore an europium centered CPL is a strong indication that also the neutral PyBox ligand is bonded to the metal.

The intensity of a CPL signal is quantified by the dissymmetry factor $g_{lum}$ defined as $2(I_L-I_R)/(I_L+I_R)$, with $I_L$ and $I_R$ being the intensities of the left and right polarized components of the emission. The CPL band associated with the magnetic $^5D_0 \rightarrow {}^7F_1$ transition shows a $g_{lum}$ factor of $\pm 3.8 \times 10^{-2}$ (positive for **SIL2S** and negative for **SIL2R**), the $g_{lum}$ factors are reported on the top of each band in Fig. 2.

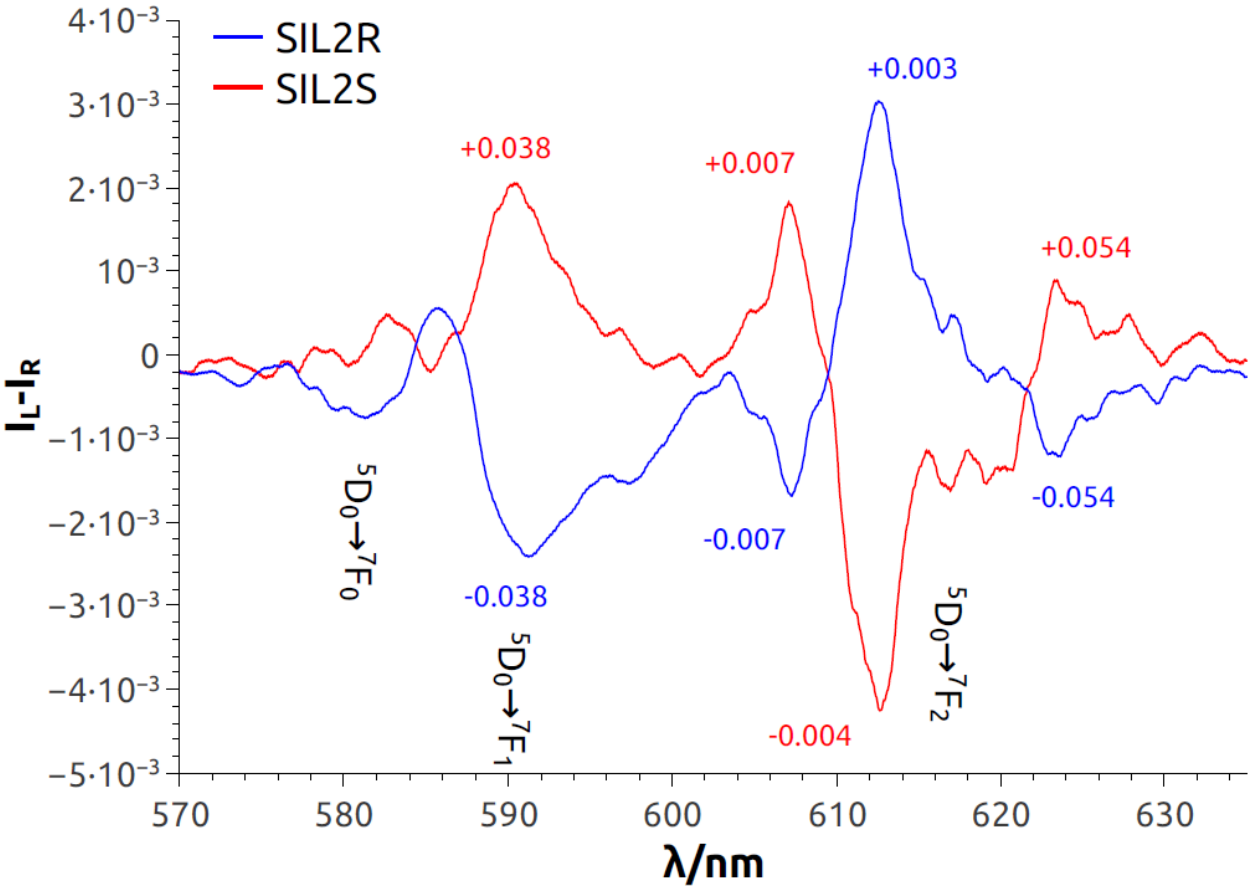


**Figure 2.** CPL spectra of **SIL2S** and **SIL2R**. Dissymmetry factors and transition assignments are shown on top of each band. The spectra are normalized to the luminescence intensitiy of the $^5D_0 \rightarrow {}^7F_2$ band taken as unity. In this way, the $g_{lum}$ value for this band corresponds to the value read on the vertical scale, while for all the other transitions they were separately calculated.

The europium derivatives **SIL2S** and **SIL2R** show a bright red emission when irradiated with ultraviolet and near visible light. Excitation spectra (Figure 3, inset) appear as broad bands centered around 370 nm with a long tail in the visible region up to 450 nm. These features are related to the coordinated dbm moieties. In fact, PyBox-based ligands are able to sensitize europium emission only through UV radiation.[23] The corresponding PL spectra, reported in Fig. 3, display the characteristic sharp bands associated to $^5D_0 \rightarrow {}^7F_J$, J = 0–4 transitions of $Eu^{3+}$ ions. Similarly to what observed in previously reported silica-based materials prepared via europium smart grafting,[8i] the spectra are dominated by the $^5D_0 \rightarrow {}^7F_2$ transition. The insertion of the chiral ligand in the complex does not modify the overall spectral profile but results in the variation of the shape and the relative intensities of the different J-manifold. Instead, the spectra of the R and S derivatives are almost identical, as expected.

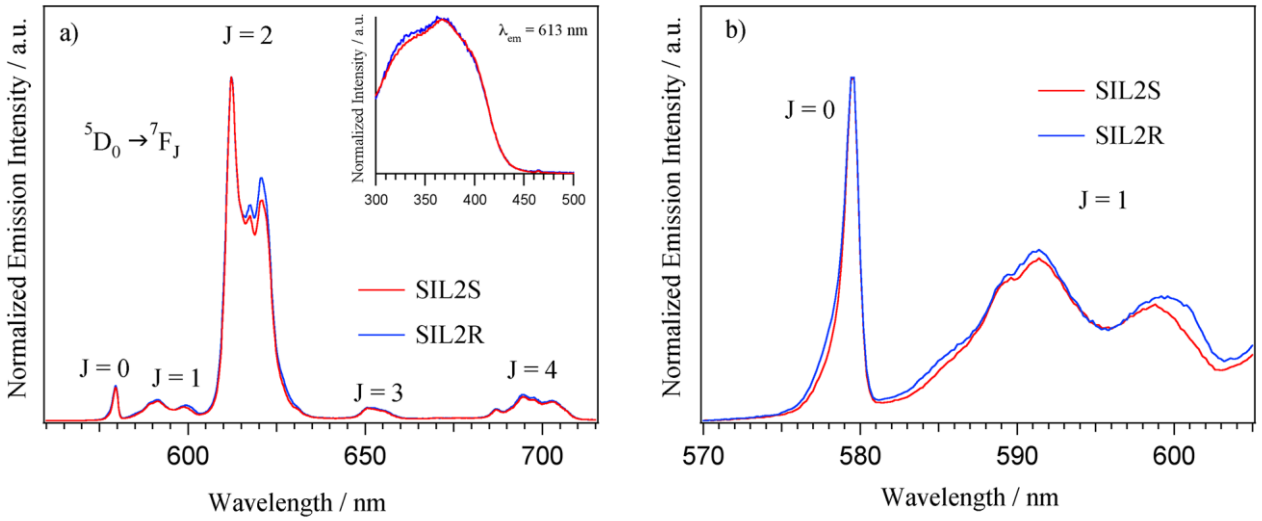


**Figure 3.** a) Room temperature emission spectra of **SIL2S** and **SIL2R** powders excited at 370 nm. Inset: Photoluminescence excitation spectra monitored on the $^5D_0 \rightarrow ^7F_0$ transition b) Expansion of the spectral region covering the $^5D_0 \rightarrow ^7F_0$ and $^5D_0 \rightarrow ^7F_1$ transitions.

As discussed above, CPL experiments showed results compatible with the presence of more than one coordination sites for europium. To this regard PL spectra can give further information. As clearly visible in Fig. 3b, the $^5D_0 \rightarrow ^7F_0$ has a tail in the low wavelength side thus suggesting the presence of at least two europium sites for which this transition is observable. In fact, due to non-degeneracy of the $^5D_0$ and $^7F_0$ levels, one peak is at maximum expected if a single emitting species is present. However, the number of non-equivalent sites can not be exactly determined from the study of $^5D_0 \rightarrow ^7F_0$ transition since this is observable only when europium ions occupy sites with particular symmetry.[24] Further evidences for multiple non-equivalent $Eu^{3+}$ centers are given by the $^5D_0 \rightarrow ^7F_1$ bands for which, on the basis of level degeneracy considerations, a maximum of three components can be observed for a single site. In our case the broad band profile is characterized by at least two maxima and two shoulders clearly indicating multiple emitting species. It is worth to note that R and S derivatives have the same behavior.

According to the previous evidences, the $^5D_0$ lifetime values were obtained by fitting the decay curves with three-exponential functions corresponding to three different $Eu^{3+}$ environments. Their average values are $\tau_{SIL2S}$ = 0.65 ms and $\tau_{SIL2R}$ = 0.69 ms.

The presence of non-equivalent $Eu^{3+}$ centers highlighted from both CPL and PL experiments is indeed expected, in view of the nature of the support. An accurate description of the amorphous silica surface properties at atomic level is difficult to obtain by experimental measurements, however some models obtained by computational methods have been reported.[25] The surface of amorphous silica exhibits silanols that can be of different types: isolated, vicinal or geminal, and their number depends on the thermal treatment that the material underwent. In the grafting process here described the surface silanols are the reactive sites affording the metal ions anchorage, so their

number and distribution is important. A simple hypothesis concerning the evolution of the system and the nature of the grafted moieties is depicted in Scheme 1, reporting anchorages of the type #SiO-Ln($O_2CNR_2$)$_2$ or (#SiO-)$_2$Ln($O_2CNR_2$), associable to reactions with isolated or vicinal silanols, respectively. In addition, a local variability in the geometry of the sites can contribute to enhance the non-equivalence of the metal centers, as for example the possibility that silicon bridging oxygen can occupy coordination sites when in favorable position.

In order to gain more insight into these materials, it was useful to compare these spectroscopic results with a molecular model system. Therefore, we synthesized the molecular enantiomeric complexes [Eu(dbm)$_3$(*S*)-$^{i}$Pr-PyBox] and [Eu(dbm)$_3$(*R*)-$^{i}$Pr-PyBox] by reacting [Eu(dbm)$_3$] with the appropriate enantiomer of $^{i}$Pr-PyBox.[8i]

Single crystal X-ray diffraction showed for both complexes a mononuclear structure with the expected composition where $^{i}$Pr-PyBox is behaving as a tridentate ligand and the europium center has coordination number nine. The asymmetric unit in the crystal structure of both enantiomers contains two independent molecules, distinguished by little conformational differences. Fig. 4 shows a sketch of the two couples of molecules and Table 2 lists the corresponding bond lengths around the metal center. The coordination polyhedron may be described as a slightly distorted capped square antiprism as shown in Fig. 5. A view of the core structure of the molecule is shown in the right side of the same figure. The sketch is traced for one of the two independent molecules of the (R) enantiomer, but it shows only little differences either with the other molecule of the (R) enantiomer or with the molecules of the (S) one. For what concerns the close surrounding of the metal, the Eu(dbm)$_3$ section of the molecules either R or S are approximately mirror symmetrical, as it can be seen looking at the Fig. 5 or Fig. 6, where the molecules are viewed along this pseudo mirror. Therefore, the dissymmetry in the coordination of the metal and the chirality are essentially due to $^{i}$Pr-PyBox ligand, which binds just on this plane. Its *iso*-propyl legs remove the mirror symmetry and define the chirality.

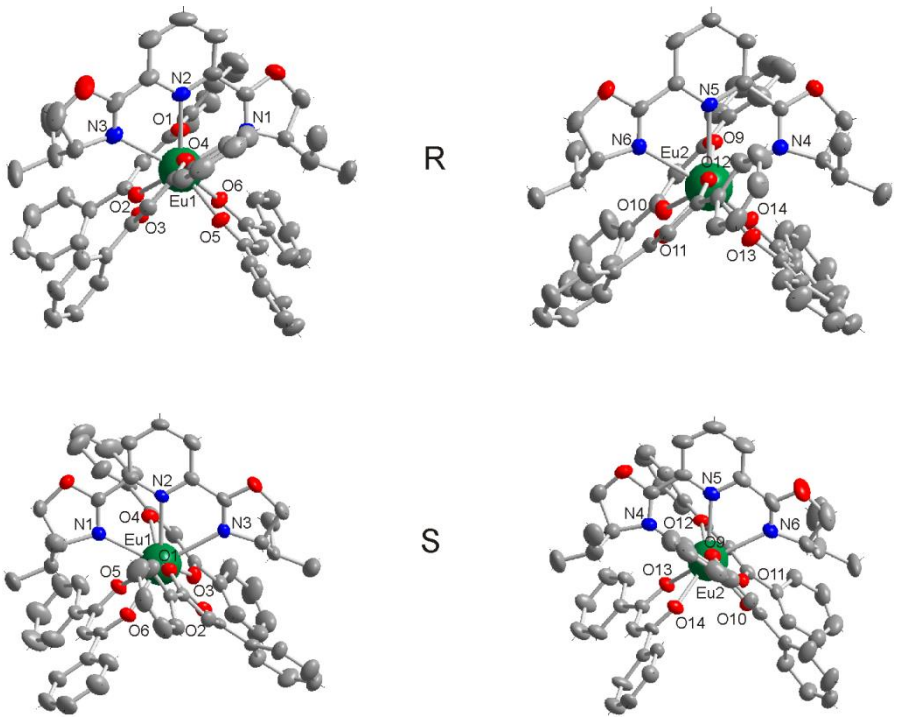


**Figure 4.** View of the two independent molecules present in the crystal structure of R Eu(dbm)$_3$(*R*)($^i$Pr-PyBox) and S Eu(dbm)$_3$(*S*)($^i$Pr-PyBox). Ellipsoids are at 50% probability. Hydrogen atoms are omitted for clarity.

**Table 2**. Selected bond lengths in the structures of Eu(dbm)$_3$($^i$Pr-PyBox)

| Eu(dbm)$_3$(*R*)($^i$Pr-PyBox) | | | | Eu(dbm)$_3$(*S*)($^i$Pr-PyBox) | | | |
|---|---|---|---|---|---|---|---|
| Eu1–N1 | 2.687(6) | Eu2–N4 | 2.685(5) | Eu1–N1 | 2.685(7) | Eu2–N4 | 2.692(8) |
| Eu1–N2 | 2.703(5) | Eu2–N5 | 2.724(4) | Eu1–N2 | 2.741(7) | Eu2–N5 | 2.703(8) |
| Eu1–N3 | 2.712(5) | Eu2–N6 | 2.738(5) | Eu1–N3 | 2.743(6) | Eu2–N6 | 2.710(7) |
| Eu1–O1 | 2.440(5) | Eu2–O9 | 2.399(5) | Eu1–O1 | 2.429(7) | Eu2–O9 | 2.392(8) |
| Eu1–O2 | 2.363(5) | Eu2–O10 | 2.378(4) | Eu1–O2 | 2.364(7) | Eu2–O10 | 2.387(6) |
| Eu1–O3 | 2.378(4) | Eu2–O11 | 2.382(5) | Eu1–O3 | 2.380(6) | Eu2–O11 | 2.369(7) |
| Eu1–O4 | 2.388(5) | Eu2–O12 | 2.430(5) | Eu1–O4 | 2.408(7) | Eu2–O12 | 2.445(7) |
| Eu1–O5 | 2.420(4) | Eu2–O13 | 2.400(4) | Eu1–O5 | 2.407(7) | Eu2–O13 | 2.383(6) |
| Eu1–O6 | 2.387(4) | Eu2–O14 | 2.397(5) | Eu1–O6 | 2.408(6) | Eu2–O14 | 2.412(7) |

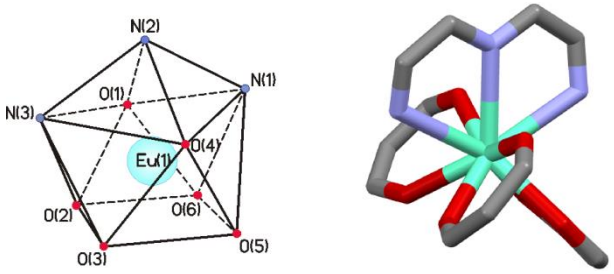


**Figure 5.** Coordination polyhedron around Eu in one of the two independent molecules of (R) Eu(dbm)$_3$($^i$Pr-PyBox) and view of the core structure of the molecule showing only minor differences either in (S) or in (R) enantiomers.

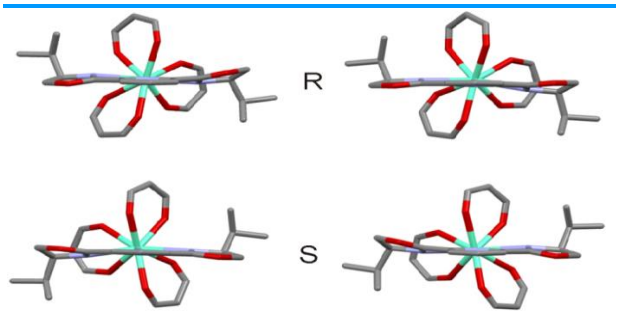


**Figure 6.** Top view of the structure of the two couples of enantiomer molecules pointing out the metal environment

In order to verify if the whole reaction product has the same crystal structure of the single crystal studied, a crop of crystals of the two enantiomeric complexes were milled and their XRD patterns were recorded. In Fig. 7 the XRD patterns of the two enantiomers are compared with the pattern calculated from the single crystal structure of one enantiomer (R). Fitting of the calculated profile was obtained by refining the background function, the profile function parameters, the sample displacement and the preferred orientation using the PowderCell program.[26] The good correspondence of the three patterns suggests that in both cases we are dealing with phase pure products.

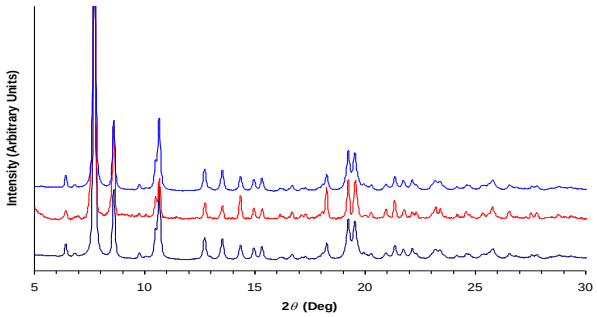


**Figure 7.** Comparison between XRD powder patterns of S (blue) and R (red) Eu(dbm)$_3$($^i$Pr-PyBox) and the pattern calculated from the single crystal structure (black).

The profiles of the emission spectra of the complexes (Fig. 8) are similar to what observed for SIL2S and SIL2R, *i.e.* the $^5D_0 \rightarrow {}^7F_2$ is the most intense transition, but all the bands appear narrower and better resolved (cfr.Fig. 3).

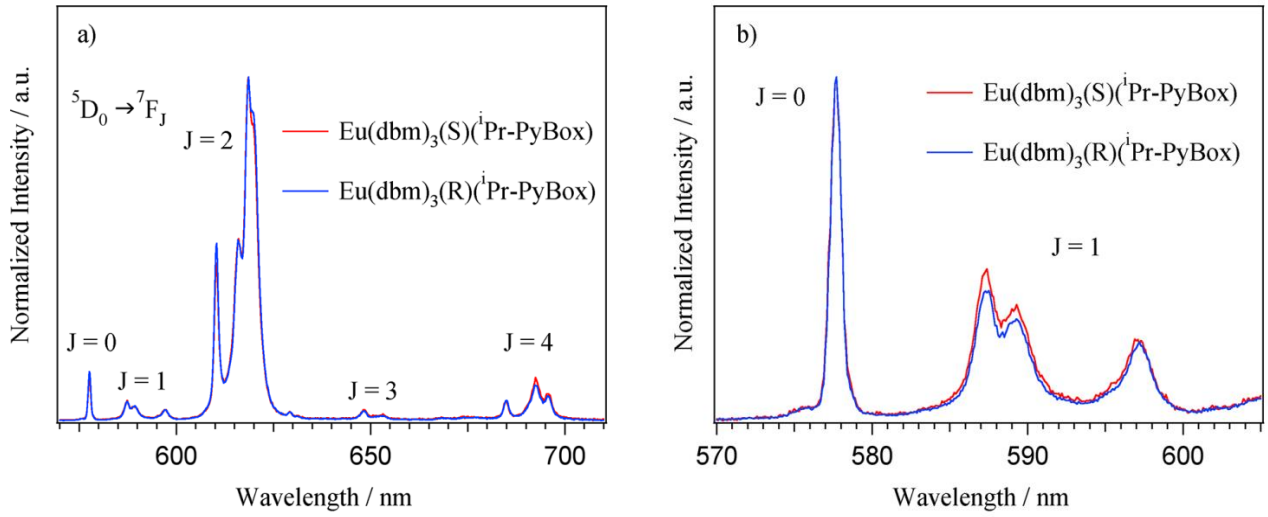


**Figure 8.** a) Room temperature emission spectra of Eu(dbm)$_3$(*S*)($^i$Pr-PyBox) and Eu(dbm)$_3$(*R*)($^i$Pr-PyBox) powders excited at 370 nm. b) Expansion of the spectral region covering the $^5D_0 \rightarrow {}^7F_0$ and $^5D_0 \rightarrow {}^7F_1$ transitions.

In this case, the $^5D_0 \rightarrow {}^7F_0$ and $^5D_0 \rightarrow {}^7F_1$ spectra are simpler and from the number of observed bands the presence of a single $Eu^{3+}$ emitting site can be deduced. This finding is confirmed by the mono-exponential profile of the decay curves ($\tau$ = 0.38 ms for both enantiomers). [Eu(dbm)$_3$(*S*)($^i$Pr-PyBox)] and [Eu(dbm)$_3$(*R*)($^i$Pr-PyBox)] have in common ligands with **SIL2S** and **SIL2R**, and all the observed differences are due to the $Eu^{3+}$ coordination sites saturated by the silica surface sites.

We recorded CPL spectra of the enantiomer molecular complexes on quartz plate depositions (Fig. 9). The obtained spectra are significantly distinct from the CPL spectra of the functionalized silica, and this is a further evidence that the coordination environment around the europium centers is completely different in the complex and on the inorganic substrate.

In the case of the molecular complex, the $g_{lum}$ values are around 3 x $10^{-2}$ for the bands associated with the $^5D_0 \rightarrow {}^7F_1$ transition and 1.2 x $10^{-2}$ and 3 x $10^{-3}$ for the bands at 614 and 619 nm, respectively. These values are of the same order of magnitude of those recorded for the grafted material.

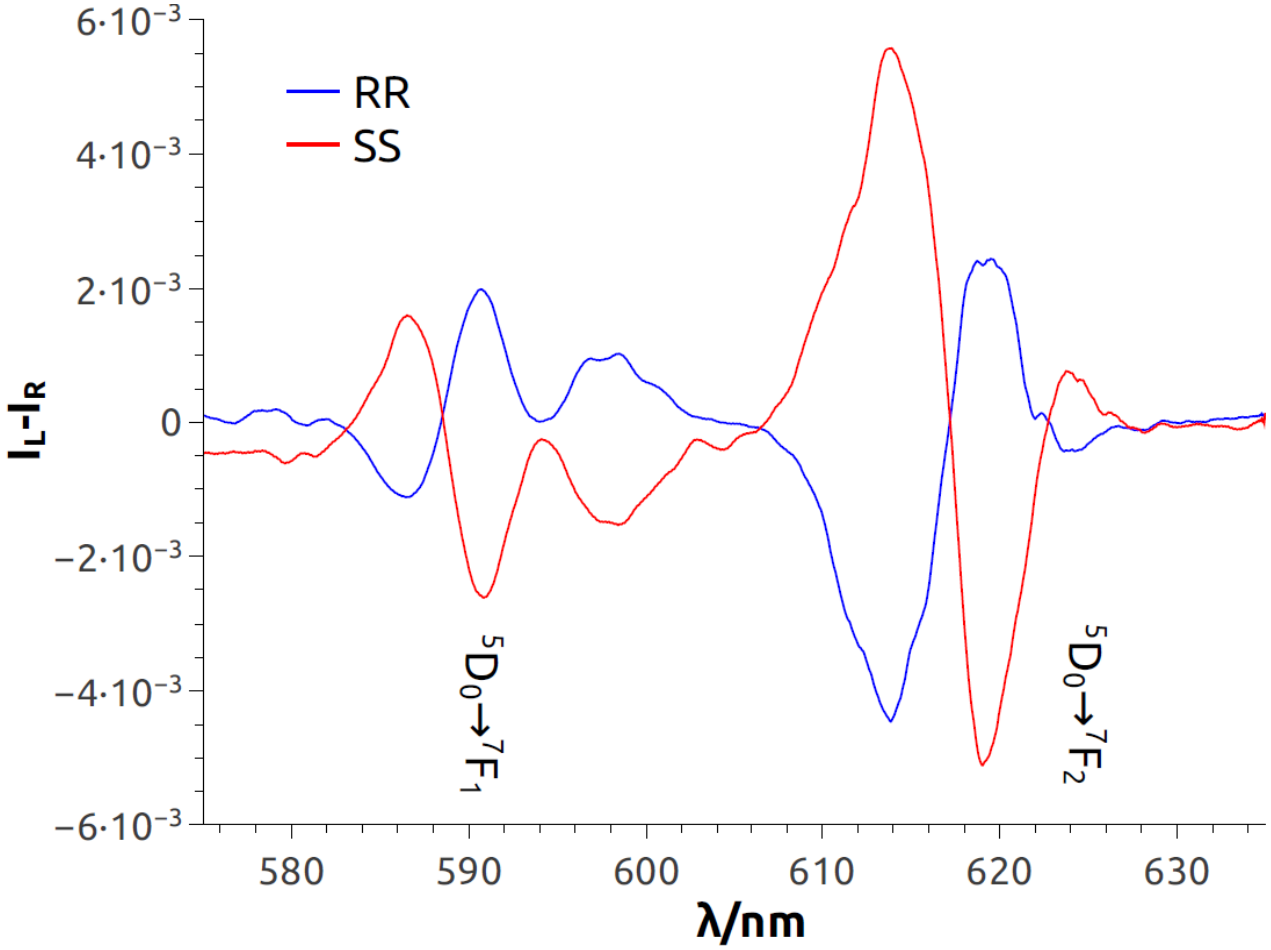


**Figure 9.** CPL spectrum of Eu(dbm)$_3$((*S*)-$^i$Pr-PyBox) and Eu(dbm)$_3$((*R*)-$^i$Pr-PyBox) on a quartz plate deposition. Transition assignments are shown on top of each band. The spectra are normalized to the luminescence intensitiy of the $^5D_0 \rightarrow {}^7F_2$ band, taken as unity. In this way, the $g_{lum}$ value for this band corresponds to the value read on the vertical scale, while for all the other transitions they were separately calculated.

## Conclusions

In this paper, the smart grafting protocol [8i] has been enriched with the further step of the sequential functionalization. We show here that after the initial grafting of europium onto commercial silica and the subsequent protolytic substitution of the residual carbamato groups, it is possible to introduce in the coordination sphere of the grafted lanthanide an additional multidentate neutral ligand in view of the availability of coordination sites. In the last step, the choice of a chiral heteroaromatic base afforded spectroscopic evidence (CPL) of the success of this sequential procedure.

In this way, for the first time, it was possible to obtain a silica material with grafted europium centers featuring highly circularly polarized luminescence. The controlled step by step introduction of suitable ligands in the coordination sphere of an initially grafted metal center is a powerful and general route to prepare multifunctional materials.

ASSOCIATED CONTENT

**Supporting Information**

The Supporting Information is available free of charge on the ACS Publications website at DOI:

…...

CPL spectra of the two enantiomers of $Eu(dbm)_3(^{i}Pr\text{-}PyBox)$ in solution ($CH_2Cl_2$, $10^{-3}$ M) are reported.

**Notes**

The authors declare no competing financial interest.

**ACKNOWLEDGMENTS**

The authors wish to thank the Università di Pisa (Fondi di Ateneo 2014 and 2015 and PRA_2016_50 Materiali Funzionali, Progetti di Ricerca di Ateneo) and Ministero Istruzione Università e Ricerca, MIUR (PRIN 2015, 20154X9ATP, Progetti di Ricerca di Interesse Nazionale) for financial support. Dr. Simona Barison and Dr. Stefania Fiameni (ICMATE CNR, Padova) are gratefully acknowledged for ICP analysis.

## Table of Content Graphics

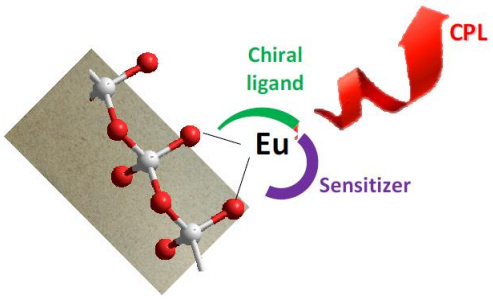


The article describes the synthesis of silica-grafted europium complexes carrying a chiral ligand. A controlled step by step substrate functionalization exploiting the reactivity of the carbamato ligands affords the first hybrid organic/inorganic material featuring circularly polarized luminescence.

## REFERENCES


[1] (a) Maas, H.; Currao, A.; Calzaferri, G. Encapsulated Lanthanides as Luminescent Materials. *Angew. Chem. Int. Ed.*, **2002**, *41*, 2495-2497. (b) Zou, J.-P.; Luo, S.-L.; Li, M.-J.; Tang, X.-H.; Xing, Q.-J.; Peng, Q.; Guo; G.-C. Syntheses, crystal structures, and magnetic and luminescent properties of a series of lanthanide coordination polymers with chelidamic acid ligand. *Polyhedron*, **2010**, *29*, 2674-2679. (c) Gallardo, H.; Conte, G.; Bortoluzzi, A. J.; Bechtold, I. H.; Pereira, A.; Quirino, W. G.; Legnani, C.; Cremona, M. Synthesis, structural characterization, and photo and electroluminescence of a novel terbium(III) complex: {Tris(acetylacetonate) [1,2,5]thiadiazolo[3,4-f][1,10] phenanthroline}terbium(III). *Inorg. Chim. Acta*, **2011**, *365*, 152-158. (d) Edelmann, F. T. Lanthanide amidinates and guanidinates in catalysis and materials science: a continuing success story. *Chem. Soc. Rev.*, **2012**, *41*, 7657-7672.

[2] (a) Inanaga, J.; Furuno, H.; Hayano, T. Asymmetric Catalysis and Amplification with Chiral Lanthanide Complexes. *Chem. Rev.*, **2002**, *102*, 2211-2226. (b) Ishitani, H.; Kobayashi, S. Catalytic asymmetric aza Diels-Alder reactions using a chiral lanthanide Lewis acid. Enantioselective synthesis of tetrahydroquinoline derivatives using a catalytic amount of a chiral source. *Tetrahedron Lett*., **1996**, *37*, 7357-7360. (c) Shibasaki, M.; Sasai, H.; Arai, T. Asymmetric Catalysis with Heterobimetallic Compounds. *Angew. Chem. Int. Ed.*, **1997**, *36*, 1236-1256. (d) Mikami, K.; Terada, M.; Matsuzawa, H.; "Asymmetric" catalysis by lanthanide complexes. *Angew. Chem. Int. Ed.*, **2002**, *41*, 3554-3571. (e) Schaus, S. E.; Jacobsen, E. N. Asymmetric Ring Opening of Meso Epoxides with TMSCN Catalyzed by (pybox)lanthanide Complexes. *Org. Lett.*, **2000**, *2*, 1001-1004. (f) Aspinall, H. C. Chiral Lanthanide Complexes: Coordination Chemistry and Applications. *Chem. Rev.*, **2002**, *102*, 1807-1850. (g) Aspinall, H. C.; Bickley, J. F.; Greeves, N.; Kelly, R. V.; Smith, P. M. Lanthanide Pybox Complexes as Catalysts for Enantioselective Silylcyanation of Aldehydes. *Organometallics*, **2005**, *24*, 3458-3467.

[3] (a) Bünzli, J.-C. G.; Piguet, C. Taking advantage of luminescent lanthanide ions. *Chem. Soc. Rev.*, **2005**, *34*, 1048-1077; (b) Binnemans, K. Lanthanide-Based Luminescent Hybrid Materials. *Chem. Rev.*, **2009**, *109*, 4283-4374; (c) Eliseeva, S. V.; Bünzli, J.-C. G. Lanthanide luminescence for functional materials and bio-sciences. *Chem. Soc. Rev.*, **2010**, *39*, 189-227; (d) Armelao, L; Quici, S.; Barigelletti, F.; Accorsi, G.; Bottaro, G.; Cavazzini, M.; Tondello, E. *Coord. Chem. Rev.*, **2010**, *254*, 487-505. (e) Bünzli, J.-C. G. On the design of highly luminescent lanthanide complexes. *Coord. Chem. Rev.*, **2015**, *293–294*, 19-47.

[4] (a) Zinna, F.; L. Di Bari, L. Lanthanide Circularly Polarized Luminescence: Bases and Applications. *Chirality* **2015**, *27*, 1-13. (b) Tsukube, H.; Shinoda, S. Lanthanide Complexes in Molecular Recognition and Chirality Sensing of Biological Substrates. *Chem. Rev.*, **2002**, *102*, 2389-2404. (c) Parker, D.; Dickins, R. S.; Puschmann, H.; Crossland, C.; Howard, J. A. K. Being Excited by Lanthanide Coordination Complexes: Aqua Species, Chirality, Excited-State Chemistry, and Exchange Dynamics. *Chem. Rev*. **2002**, *102*, 1977-2010.

[5] a) Lunkley, J. L.; Shirotani, D.; Yamanari, K.; Kaizaki, S.; Muller, G. Chiroptical Spectra of a Series of Tetrakis((+)-3-heptafluorobutylyrylcamphorato)lanthanide(III) with an Encapsulated Alkali Metal Ion: Circularly Polarized Luminescence and Absolute Chiral Structures for the Eu(III) and Sm(III) Complexes. *Inorg. Chem.* **2011,** *50*, 12724-12732. b) Zinna, F.; Resta, C.; Abbate, S.; Castiglioni, E.; Longhi, G.; Mineo, P.; Di Bari, L. Circularly polarized luminescence under near-UV excitation and structural elucidation of a Eu complex. *Chem.Commun.*, **2015**, *51*, 11903-11906.

[6] a) Muller, G. Luminescent chiral lanthanide(III) complexes as potential molecular probes. *Dalton Trans.*, **2009**, 9692-9707. b) Montgomery, C. P.; Murray, B. S.; New, E. J.; Pal, R.; Parker, D. Cell-Penetrating Metal Complex Optical Probes: Targeted and Responsive Systems Based on Lanthanide Luminescence. *Acc. Chem. Res.*, **2009**, *42*, 925-937. c) Carr, R.; Evans, N. H.; Parker, D. Lanthanide complexes as chiral probes exploiting circularly polarized luminescence. *Chem. Soc. Rev.*, **2012**, *41*, 7673-7686.

[7] a) Zinna, F.; Giovanella, U.; Di Bari, L. Highly Circularly Polarized Electroluminescence from a Chiral Europium Complex. *Adv. Mater.*, **2015**, *27*, 1791-1795. b) Zinna, F.; Pasini, M.; Galeotti, F.; Botta, C.; Di Bari, L.; Giovanella, U. Design of Lanthanide-Based OLEDs with Remarkable Circularly Polarized Electroluminescence. *Adv. Funct. Mater.* **2016**, 10.1002/adfm.201603719 .

[8] (a) Abis, L.; Belli Dell'Amico, D.; Busetto, C.; Calderazzo, F.; Caminiti, R.; Ciofi, C.; Garbassi, F.; Masciarelli, G. ***N,N***-Dialkylcarbamato complexes as precursors for the chemical implantation of metal cations on a silica support. *J. Mater. Chem.* **1998**, *8*, 751-759. (b) Abis, L.; Belli Dell'Amico, D.; Busetto, C.; Calderazzo, F.; Caminiti, R.; Garbassi, F.; Tomei, A. ***N,N***-Dialkylcarbamato complexes as precursors for the chemical implantation of metal cations on a silica support. Part 3 Palladium. *J. Mater. Chem.* **1998**, *8*, 2855-2861. (c) Abis, L.; Maichle-Mössmer, C.; Calderazzo, F.; Pampaloni, G.; Strähle, J.; Tripepi, G. Cyclopentadienyl–diethylcarbamato derivatives of zirconium(IV) and hafnium(IV), $[M(C_5H_5)(O_2CNEt_2)_3]$: synthesis and use as precursors for chemical implantation on a silica surface. *J. Chem. Soc., Dalton Trans*. **1998**, 841-845. (d) Belli Dell'Amico, D.; Lora, S.; D'Archivio, A. A.; Galantini, L.; Biffis, A.; Corain, B. Metal ion implantation onto acidic resins upon reaction of metal acetates and carbamates: Part I. Synthetic results. *J. Mol. Catal. A: Chem*., **2000**, *157*, 173-181. (e) Abis, L.; Armelao, L.; Belli Dell'Amico, D.;

Calderazzo, F.; Garbassi, F.; Merigo, A.; Quadrelli, E. A. Gold molecular precursors and gold–silica interactions. *J. Chem. Soc., Dalton Trans.*, **2001**, 2704-2709. (f) Belli Dell'Amico, D.; Calderazzo, F.; Labella, L.; Marchetti, F.; Pampaloni, G. *N,N*-dialkylcarbamato metal complexes, molecular inorganic precursors to functionalized inorganic matrices. *Inorg. Chem. Commun.* **2002**, *5*, 733-745. (g) Abis, L.; Belli Dell' Amico, D.; Calderazzo, F.; Caminiti, R.; Garbassi, F.; Ianelli, S.; Pelizzi, G.; Robino, P.; Tomei, A. *J. Mol. Catal. A: Chem*., **1996**, *108*, L113-L117. (h) Armelao, L.; Belli Dell'Amico, D.; Bellucci, L.; Bottaro, G.; Labella, L.; Marchetti, F.; Samaritani S. Smart Grafting of Lanthanides onto Silica via *N,N*-Dialkylcarbamato Complexes. *Inorg. Chem.*, **2016**, *55*, 939-947.

[9] (a) Anwander, R. SOMC@PMS. Surface Organometallic Chemistry at Periodic Mesoporous Silica. *Chem. Mater*., **2001**, *13*, 4419-4438. (b) Liang, Y.; Anwander, R. Nanostructured catalysts ***via*** metal amide-promoted smart grafting. *Dalton Trans*. **2013**, *42*, 12521-12545. (c) Copéret, C.; Basset, J.-M. Strategies to Immobilize Well-Defined Olefin Metathesis Catalysts: Supported Homogeneous Catalysis *vs.* Surface Organometallic Chemistry. *Adv. Synth. Catal*. **2007**, *349*, 78-92. (d) Dorcier, A.; Merle, N.; Taoufik, M.; Bayard, F.; Lucas, C.; de Mallmann, A.; Basset, J.-M. Preparation of a Well-Defined Silica-Supported Nickel-Diimine Alkyl Complex − Application for the Gas-Phase Polymerization of Ethylene. *Organometallics* **2009**, *28*, 2173-2178. (e) Gu, W.; Stalzer, M. M.; Nicholas, C. P.; Bhattacharyya, A.; Motta, A.; Gallagher, J. R.; Zhang, G.; Miller, J. T.; Kobayashi, T.; Pruski, M.; Delferro, M.; Marks, T. J. Benzene Selectivity in Competitive Arene Hydrogenation: Effects of Single-Site Catalyst·Acidic Oxide Surface Binding Geometry. *J. Am. Chem. Soc*. **2015**, *137*, 6770-6780. (f) Chen, Y.; Abou-hamad, E.; Hamieh, A.; Hamzaoui, B.; Emsley, L.; Basset, J.-M. Alkane Metathesis with the Tantalum Methylidene $[(\equiv SiO)Ta(=CH_2)Me_2]/[(\equiv SiO)_2Ta(=CH_2)Me]$ Generated from Well-Defined Surface Organometallic Complex $[(\equiv SiO)Ta^{V}Me_4]$. *J. Am. Chem. Soc*. **2015**, *137*, 588-591. (g) Le Roux, E.; Anwander, R. *Modern Surface Organometallic Chemistry* **2009**, Wiley, 455-512. (h) Lapadula, G.; Bourdolle, A.; Allouche, F.; Conley, M. P.; del Rosal, I.; Maron, L.; Lukens, W. W.; Guyot, Y.; Andraud, C.; Brasselet, S.; Copéret, C.; Maury, O.; Andersen, R. A. Near-IR Two Photon Microscopy Imaging of Silica Nanoparticles Functionalized with Isolated Sensitized Yb(III) Centers. *Chem. Mater*. **2014**, *26*, 1062-1073. (i) Copéret C., Comas-Vives A., Conley M. P., Estes D. P., Fedorov A., Mougel V., Nagae H., Núñez-Zarur F., Zhizhko P. A. Surface Organometallic and Coordination Chemistry toward Single-Site Heterogeneous Catalysts: Strategies, Methods, Structures, and Activities. *Chem. Rev*. **2016**, *116*, 323-421.

[10] Belli Dell'Amico, D.; Calderazzo, F.; Labella, L.; Marchetti, F.; Pampaloni, G. Converting Carbon Dioxide into Carbamato Derivatives. *Chem. Rev*. **2003**, *103*, 3857-3898.

[11] Tohgha, U.; Deol, K. K.; Porter, A. G.; Bartko, S. G.; Choi, J. K.; Leonard, B. M.; Varga, K.; Kubelka, J.; Muller, G.; Balaz, M. Ligand Induced Circular Dichroism and Circularly Polarized Luminescence in CdSe Quantum Dots. *ACS Nano*, **2013**, *7*, 11094-11102.

[12] Morita, M.; Rau, D.; Kai, T. Luminescence and circularly polarized luminescence of macrocyclic Eu(III) and Tb(III) complexes embedded in xerogel and sol–gel $SiO_2$ glasses. *J. Lumin.*, **2002**, *100*, 97-106.

[13] Brunet, E.; Jiménez, L.; Victoria-Rodriguez, M.; Luu, V.; Muller, G.; Juanes, O.; Rodríguez-Ubis, J. C. The use of lanthanide luminescence as a reporter in the solid state: Desymmetrization of the prochiral layers of γ-zirconium phosphate/phosphonate and circularly polarized luminescence. *Micropor. Mesopor. Mat.*, **2013**,*169*, 222-234.

[14] Armelao, L.; Belli Dell'Amico, D.; Biagini, P.; Bottaro, G.; Chiaberge, S.; Falvo, P.; Labella, L.; Marchetti, F.; Samaritani, S. Preparation of *N,N*-Dialkylcarbamato Lanthanide Complexes by Extraction of Lanthanide Ions from Aqueous Solution into Hydrocarbons. *Inorg. Chem*. **2014**, *53*, 4861-4871.

[15] Yu, L.; Chen, D.; Li, J.; Wang, P. G. Preparation, Characterization, and Synthetic Uses of Lanthanide(III) Catalysts Supported on Ion Exchange Resins. *J. Org. Chem*. **1997**, *62*, 3575-3581.

[16] Zinna, F.; Bruhn, T.; Guido, C. A.; Ahrens, J.; Bröring, M.; Di Bari, L.; Pescitelli, G. *Chem. Eur. J.*, **2016**, doi: 10.1002/chem.201602684.

[17] *APEX2*. Version 2014.11-0; Bruker-AXS Inc.: Madison, Wisconsin, USA, **2014**.

[18] Sheldrick, G. M. (2013). *SHELXS*. Version 2014/7. Georg-August-Universität Göttingen, Göttingen, Germany.

([19])Sheldrick, G. M.; *SHELXL, Programs for Crystal Structure Analysis (Release 97-2)*, Georg-August-Universität Göttingen, Göttingen, Germany, **1998**.

([20])Farrugia, L. J. *WinGX* suite for small-molecule single-crystal crystallography. *J. Appl. Crystallogr.*, **1999**, *32*, 837-838.

[21] (a) De Silva, C. R.; Wang, J.; Carducci, M. D.; Rajapakshe, S. A.; Zheng, Z. Synthesis, structural characterization and luminescence studies of a novel europium(III) complex $[Eu(DBM)_3(TPTZ)]$ (DBM: dibenzoylmethanate; TPTZ: 2,4,6-tri(2-pyridyl)-1,3,5-triazine). *Inorg. Chim. Acta* **2004**, *357*, 630-634. (b) Kirby, A. F.; Richardson, F. S. Detailed analysis of the optical absorption and emission spectra of europium(3+) in the trigonal (C3) $Eu(DBM)_3{\cdot}H_2O$ system. *J. Phys. Chem.* **1983**, *87*, 2544-2556. (c) Li, X. L.; Gao, Y. L.; Feng, X. L.; Zheng, Y. X.; Chen, C. L.; Zuo, J. L.; Fang, S. M. Two mono- and dinuclear Eu(III) enantiomeric pairs based on chiral bis-bidentate bridging ligands: synthesis, structures, luminescent and ferroelectric properties. *Dalton Trans.* **2012**, *41*, 11829-11835.

[22] (a) Yuasa, J.; Ohno, T.; Miyata, K.; Tsumatori, H.; Hasegawa, Y.; Kawai, T. Noncovalent Ligand-to-Ligand Interactions Alter Sense of Optical Chirality in Luminescent Tris(β-diketonate) Lanthanide(III) Complexes Containing a Chiral Bis(oxazolinyl) Pyridine Ligand. *J. Am. Chem. Soc*., **2011**, *133*, 9892-9902. (b) Harada, T.; Nakano, Y.; Fujiki, M.; Naito, M.; Kawai, T.; Hasegawa, Y. Circularly Polarized Luminescence of Eu(III) Complexes with Point- and Axis-Chiral Ligands Dependent on Coordination Structures. *Inorg. Chem*. **2009**, *48*, 11242-11250.

[23] Matsumoto, K.; Suzuki, K.; Tsukuda, T.; Tsubomura T. A Chiral 2,6-Bis(Oxazolinyl)Pyridine Ligand with Amide Groups to Form Isomorphous Complexes through All the Lanthanoid Series. *Inorg. Chem.* **2010**, *49*, 4717-4719.

[24] (a) Binnemans, K.; Interpretation of europium(III) spectra. *Coord. Chem. Rev.* **2015**, *295*, 1-45. (b) Tanner P. A. Some misconceptions concerning the electronic spectra of tri-positive europium and cerium. *Chem. Soc. Rev.* **2013**, *42*, 5090-5101.

[25] (a) Zhuravlev, L.T. The surface chemistry of amorphous silica. Zhuravlev model, *Colloids and SurfacesA: Physicochemical and Engineering Aspects* **2000**, *173*, 1-38. (b) Ewing, C. S.; Bhavsar, S.; Gӧtz, V.; McCarthy, J. J.; Johnson, J. K. Accurate Amorphous Silica Surface Models from First-Principles Thermodynamics of Surface Dehydroxylation. *Langmuir* **2014**, *30*, 5133-5141.

[26] Kraus, W.; Nolze, G. PowderCell rel. 2.4, Program for manipulating powder patterns, Berlin, 2000.